

A Robust Technique for Optical OFDM Systems in Clipping Noise Mitigation

T.D.N.S.S.Sarveswara Rao, Assistant Professor

Department of Electronics and Communication Engineering,

Sri Vasavi Engineering College Tadepalligudem, Andhra Pradesh, INDIA

Email ID: tdnssr Rao@gmail.com

ABSTRACT

This letter portrays another non-straight calculation for cut-out clamor relief in force regulation/coordinate discovery dc one-sided optical symmetrical recurrence division multiplexing (DCO-OFDM) frameworks. Cut-out commotion is frequently the significant constraint in DCO-OFDM. In this letter, we demonstrate that additional data about the cut flag can be extricated utilizing a non-direct process and afterward used to alleviate the cut-out clamor. The adequacy of the new calculation is shown by recreation and in an optical remote trial.

Index Terms— Intensity modulation/direct detection (IM/DD), optical OFDM, clipping noise.

I. INTRODUCTION

Orthogonal frequency division multiplexing (OFDM) is increasingly being considered as a modulation technique for intensity modulated/direct detection (IM/DD) optical wireless communication (OWC) systems [1], [2]. In IM/DD systems, the transmitted signals are modulated onto the intensity of the light and thus have to be unipolar. To make a conventional bipolar OFDM signal into a unipolar signal, one popular approach [2] is to add a dc bias and then clip the OFDM signal at zero. However, for low bias levels, clipping introduces significant distortion which can lead to data detection errors [3].

In this letter we describe a new algorithm for mitigating clipping noise in OFDM and show both experimentally and by simulation that it can significantly improve performance in an IM/DD system. In the algorithm the data is detected and used to regenerate an equivalent time domain signal which is then used to estimate the component of the

signal removed by clipping. This is combined with the Original received signal and then input into a conventional OFDM receiver.

A closely related algorithm was described in [4] for radio frequency (RF) systems, but in [4] the compensation for constellation shrinkage is not optimal and this significantly reduces the effectiveness of clipping mitigation. The new contributions in this letter include:

- A new clipping mitigation algorithm which optimally corrects for constellation shrinkage,
- Demonstration of the effectiveness of the algorithm in an IM/DD system both by simulation and experimentally on a visible light communications (VLC) testbed,
- Results for the case where different levels of clipping are used for the top and bottom of the signal.

In the following, we first analyze the effect of single-sided clipping on DCO-OFDM and show how both the shrinkage and the clipping noise level depend on the bias level. Simulation results for a number of constellation sizes and bias levels show the effect of clipping alone, and clipping plus additive white Gaussian noise (AWGN). The algorithm is then extended to double-sided clipping. Finally, a VLC experiment is used to demonstrate the algorithm in practical applications.

II. SYSTEM DESCRIPTION

A. DC-Biased Optical OFDM (DCO-OFDM)

A typical DCO-OFDM transmitter is shown in Fig. 1. The data is mapped onto the bipolar complex QAM symbols, $X = X_0, X_1, \dots, X_{N-1}$, where N is the number of subcarriers, $X_0 = X_{N/2} = 0$, and X_k is constrained to have Hermitian symmetry, so $X_k = X_{N-k}^*$ for $0 < k < N/2$. X is then input to an IFFT to give the time domain signal sequence

$$x_m = \frac{1}{\sqrt{N}} \sum_{k=0}^{N-1} X_k \exp\left\{\frac{j2\pi km}{N}\right\} \quad (1)$$

Due to the central limit theorem, x_m is approximately zero mean with Gaussian distribution so

$$P_x = \mathcal{N}(x; 0, \sigma^2) \triangleq \frac{1}{\sqrt{2\pi\sigma}} \exp\left\{-\frac{x^2}{2\sigma^2}\right\} \quad (2)$$

where σ^2 is the variance. Next, x_m is clipped at the level of $-B_{DC}$ to generate $x_{clip,m}$ where B_{DC} is a dc bias which is added at the next step to generate a positive signal. We set $B_{DC} = \mu \sqrt{E x_m^2}$ and the bias level in dB is defined as $10 \log_{10} \mu^2 + 1$ dB [3]. The clipped time domain signal sequence with the added dc bias is given by

$$s_{DCO,m} = \begin{cases} 0, & x_m < -B_{DC} \\ x_m + B_{DC}, & x_m \geq -B_{DC} \end{cases} \quad (3)$$

A cyclic prefix (CP) is then added and a digital-to-analog converter (DAC) converts the discrete signal sequence into an analog signal, $s_{DCO}(t)$. The real positive signal, $s_{DCO}(t)$, is then used to drive a LED.

B. Signal Distortion

From Clipping Operation The clipping operation in (3) both attenuates the signal and causes clipping noise. The clipped signal is given by

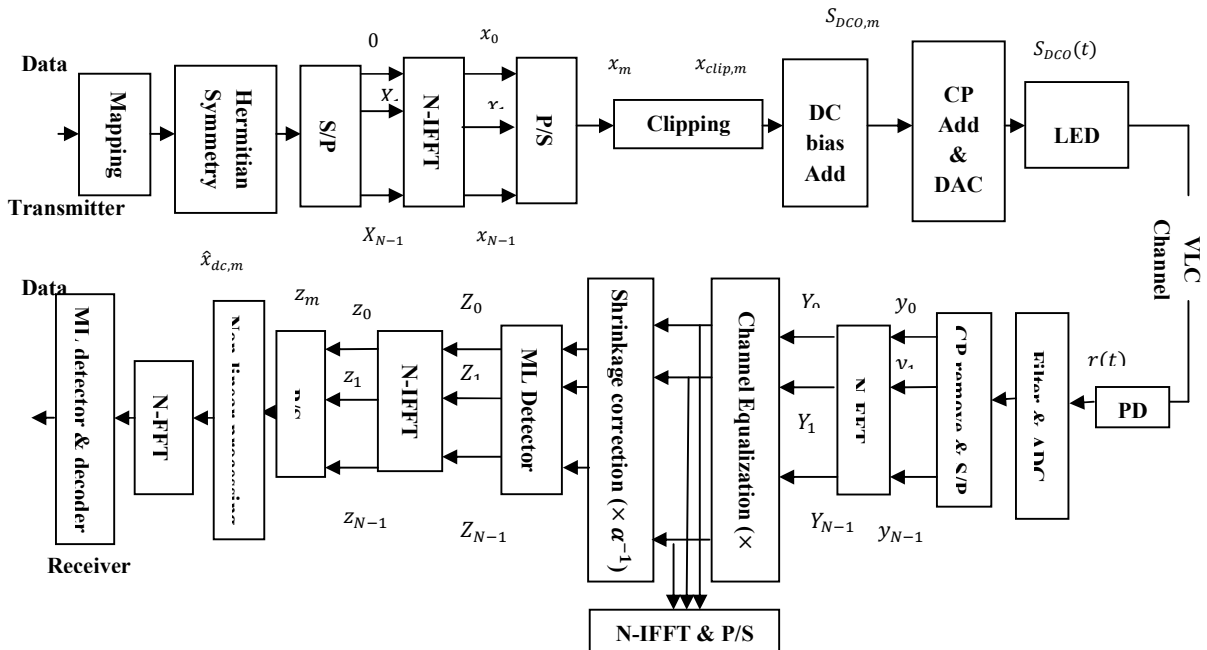


Fig.1. the structure of transmitter and receiver.

$$x_{clip,m} = x_m - x_{c,m} = \alpha x_m + c_m \quad (4)$$

where $x_{c,m}$ is the signal removed in the clipping operation, α is the attenuation factor which describes the shrinkage and c_m is the clipping noise component. Thus, by applying Busgang's theory [5],

[6], we can show and $Q(\xi) = \int_0^\xi \frac{1}{\sqrt{2\pi}} \exp(-u^2/2) du$. The variance of c_m is given by [7]:

$$\alpha = \frac{E\{x_{clip,m}x_m\}}{E\{x_mx_m\}} = \frac{1}{\sigma^2} \int_{-\infty}^{+\infty} x_{clip,m} \cdot x_m \cdot p_x(x) dx = 1 - Q(B_{DC}/\sigma) = 1 - Q(\mu), \quad (5)$$

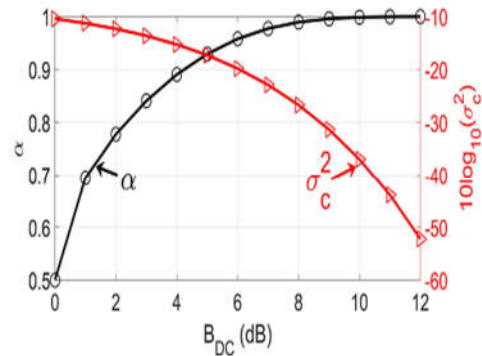


Fig.2. Attenuation and clipping noise variance versus dc bias level (dB).

$$\sigma_c^2 = \sigma^2 \left\{ (1 + \mu^2)[Q(\mu) - Q^2(\mu)] - \frac{1}{2\pi} e^{-\mu^2} - \frac{\mu}{\sqrt{2\pi}} e^{-\frac{\mu^2}{2}} [1 - 2Q(\mu)] \right\} \quad (6)$$

From (5) and (6), we can see that α is a function only of the bias level, but that σ_c^2 depends on both the bias level and σ^2 . In Fig. 2, α and σ_c^2 are plotted as a function of BDC with $\sigma^2 = 1$. It can be seen that as BDC becomes larger α increases and σ_c^2 decreases. As the bias level increases α approaches unity and σ_c^2 becomes very small.

We now describe the effects of clipping noise in the frequency domain and study its influence on BER performance. Shrinkage affects all of the subcarriers equally and results from a reduction in the overall signal power after clipping. Fig. 3 (a) shows the signal constellation after clipping for OFDM with 256 subcarriers and 4-QAM with a bias of 2 dB. We can see that the clipping noise is significant and that due to the effect of shrinkage, the centers of the constellation symbols are not at the constellation points before clipping, which are at the intersections of the dashed lines. Fig. 3 (d) shows the equivalent results for 16-QAM with a bias of 4dB. Because of the larger bias, both the shrinkage and clipping noise are less in (d) than (a). Without any correction for shrinkage, or clipping noise mitigation, these constellations would result in BERs of 5.78×10^{-4} for the 4-QAM case and 1.3×10^{-2} for the 16-QAM.

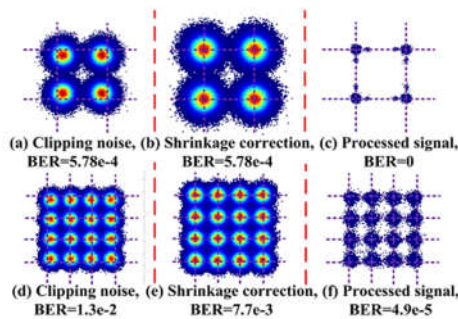


Fig.3. Signal constellation: (a) 4-QAM, after clipping, (b) 4-QAM, after shrinkage correction, (c) 4-QAM, after clipping noise mitigation, (d) 16-QAM, after clipping operation, (e) 16-QAM, after shrinkage correction, (f) 16-QAM, after clipping noise mitigation.

C. Clipping Noise Mitigation Algorithm

The clipping noise mitigation algorithm is shown in Fig. 1 and operates as follows:

- 1) The signal received by the photo detector (PD) is first filtered, converted from analog to digital and input to an FFT to give, $Y = Y_0, Y_1, \dots, Y_{N-1}$.
- 2) The elements of Y are equalized using h_k , the channel gain for each subcarrier, to give $Y_k = h^{-1} Y_k$, which is then converted back to the discrete time domain to give y_m .
- 3) The shrinkage is then corrected to give $\tilde{y}_k = \alpha^{-1} Y_k$.
- 4) \tilde{y}_k is then input into a ML detector to give output $Z_k = \arg \min_{M \in \{M-QAM\}} |\tilde{y}_k - M|^2$.
- 5) An IFFT then converts Z_k into the time domain sequence, z_m . Note that in general the samples in $z = z_0, z_1, \dots, z_{N-1}$ will have both positive and negative values.
- 6) y_m and z_m are used to generate a new time domain sequence, $\hat{x}_{dc, m}$, which is used to estimate $x_m + BDC$. It is generated by using the positive values of y_m combined with the negative values of z_m for the samples where y_m is negative or zero:

$$\hat{x}_{dc, m} = \begin{cases} y'_m, z'_m > 0 \\ z'_m, z'_m \leq 0 \end{cases} \quad (7)$$

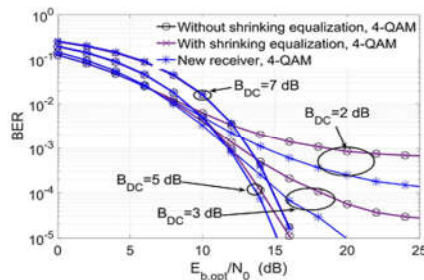


Fig.4. Comparison between conventional receivers (with and without shrinkage correction) and clipping noise mitigation receiver using 4-QAM.

In this signal reconstruction process, when $y_m > 0$, y_m is used to estimate $x_m + BDC$, and when $y_m \leq 0$, z_m is used to estimate $x_m + BDC$. This is because when clipping noise, rather than AWGN, is the dominant impairment, y_m is a better estimate for the positive parts of $x_m + BDC$ than z_m . However for the negative parts, z_m is a better estimate than y_m , as the negative parts of y_m consist of only noise.

7) Finally $\hat{x}_{dc, m}$ is input to an FFT from which the transmitted data is recovered using a ML detector.

Note that both channel equalization and shrinkage correction are used in generating z_m , but that only channel equalization is used in generating y_m .

This is because, as can be seen in (4), $x_{c,m}$ is not affected by shrinkage.

III. SYSTEM PERFORMANCE

A. Performance with Clipping Noise

Only First, we analyze the algorithm's performance when there is no AWGN, so the only impairments are shrinkage and clipping noise. Fig. 3 (b) and (e) show the constellations after shrinkage correction. Compared with the BERs in Fig. 3 (a) and (d), 4-QAM has the same BER and 16-QAM has a lower BER. This is because for 4-QAM the information is carried only on the phase not the amplitude of the subcarrier, so shrinkage does not affect the BER. For any higher order modulation the shrinkage significantly affects performance. Fig. 3 (c) and (f) show the constellations after clipping noise mitigation. The BER is reduced to 0 for 4-QAM and to 4.9×10^{-5} for 16-QAM.

B. Performance in AWGN Channel

We now study the performance of different receivers in an AWGN channel. Fig. 4 and Fig. 5 show simulation results for BER as a function of $E_{b,opt}N_0$ for 4-QAM and 16-QAM, where $E_{b,opt} = P_{opt}b$. P_{opt} is the transmitted optical power of the LED which is set to unity. b is the data rate and N_0 is the single-sided power density of the noise. The performance for all cases depends on the bias level. For a low bias, clipping noise dominates and the BER plateaus for all forms of receiver and both 4-QAM and 16-QAM. As noted above, correcting for constellation shrinkage gives no improvement for 4-QAM but gives significant improvement for 16-QAM.

Fig. 4 and 5 show that applying clipping noise mitigation significantly improves the performance for low bias levels, with the greatest improvement for low biases and high SNR.

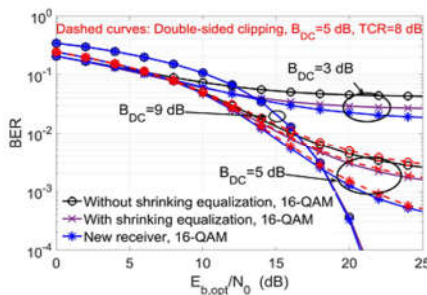


Fig.5. Comparison between conventional receivers (with and without shrinkage correction) and clipping noise mitigation receiver using 16-QAM.

However there is little improvement for bias levels >7 dB for 4-QAM or >9 dB for 16-QAM. This is because, as shown in Fig. 2, for high bias levels the variance of the clipping noise is very small.

C. Performance for Double-Sided Clipping

In practice to limit its dynamic range, the transmitted signal may be clipped at the top as well as the bottom. Our algorithm can be successfully adapted to this situation. The signal after double-sided clipping can be denoted by

$$S_{T-DCO,m} = \begin{cases} 0, & x_m < -B_{DC} \\ x_m + B_{DC}, & -B_{DC} \leq x_m \leq \lambda - B_{DC} \\ \lambda, & x_m > \lambda - B_{DC} \end{cases} \quad (8)$$

Where λ is the level at which the top of the signal is clipped. A top clipping ratio (TCR) is then defined as $20 \log_{10}(\lambda - B_{DC}) \sigma$ dB. Note that λ is typically very high [8]. In this case the attenuation is given by

$$\alpha_T = 1 - Q\left(\frac{B_{DC}}{\sigma}\right) - Q\left(\frac{\lambda - B_{DC}}{\sigma}\right) \quad (9)$$

Our algorithm can be adapted to this situation by generating the reconstructed time domain signal using

$$\hat{x}_{dc,m} = \begin{cases} z_m, & y'_m \leq 0 \\ y'_m, & 0 < y'_m < \lambda \\ z_m, & y'_m \geq \lambda \end{cases} \quad (10)$$

The performance of the algorithm applied to double-sided clipping is shown in Fig. 5 using dashed lines. We can see that the algorithm can be successfully applied to double sided clipping. The new receiver outperforms the conventional receiver with several decibels. When $TCR = 8$ dB, the clipping of the top of the signal has negligible effect on performance. However, the algorithm is completely general and will also apply where clipping at the top is more severe than clipping at the bottom and if the lower clipping level is not zero.

D. Performance with Multiple Stages Processor

We now extend the clipping noise algorithm by using multiple stage iteration. Fig. 6 shows the receiver structure with L stages. The output signal at the l th stage processor, $\hat{x}^{(l)}_{dc,m}$, is sent into the next stage and then combined with the original received signal sequence, y_m , using (7). The final reconstructed time domain sequence, $\hat{x}^{dc,(L)}_m$, is converted into the frequency domain and detected using ML decoder. Note that the channel equalization step is only performed in the first stage. Fig. 7 shows the BER results using receivers

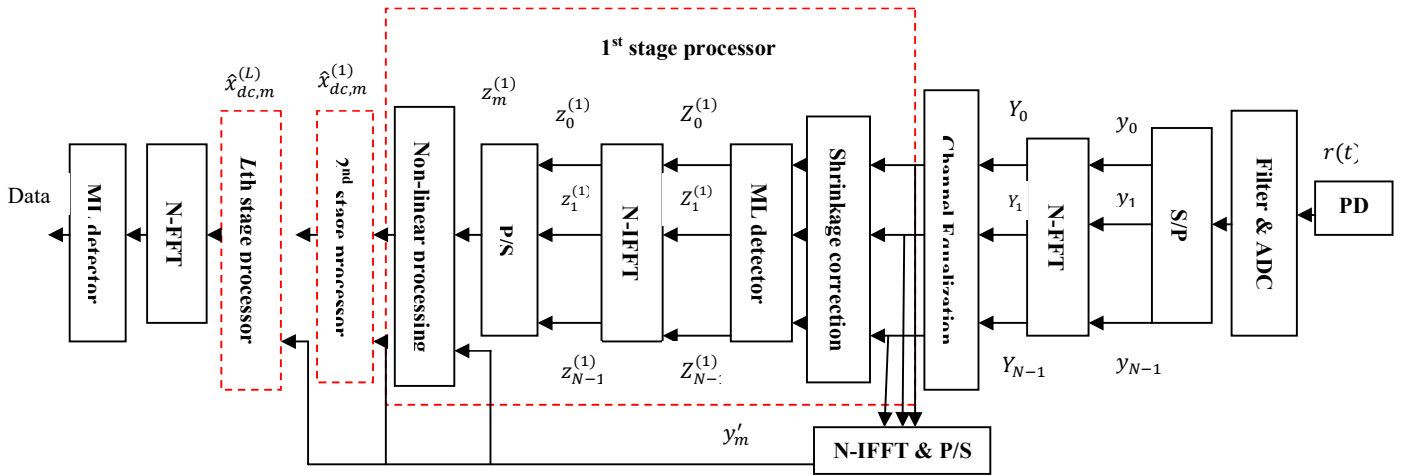


Fig. 6. Multiple stage non-linear processing receiver.

with different numbers of stages. While the first stage provides significant improvement, adding further stages has very little effect.

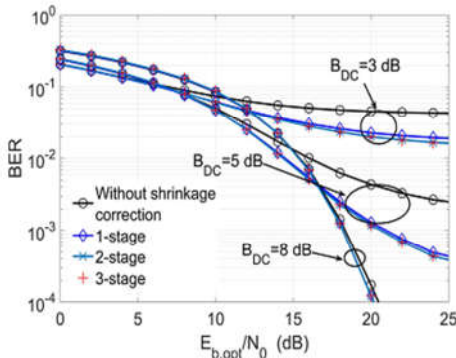


Fig. 7. BER performance using multiple stage clipping noise mitigation processor (16-QAM).

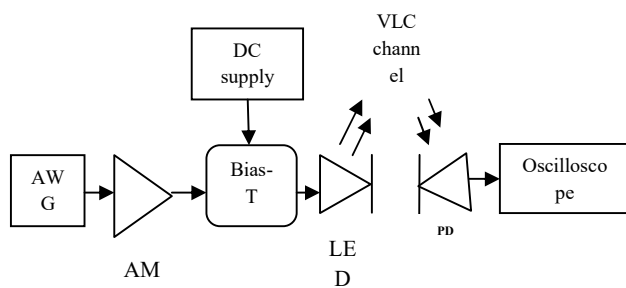


Fig.8. Experimental setup.

IV. EXPERIMENTAL RESULTS

Fig. 8 shows our VLC experimental setup. The transmitted DCO-OFDM signal with $N = 256$ and a CP length of 32 was first generated in MATLAB, and then uploaded into the arbitrary waveform

generator (AWG, Tektronix 3022B). The input signal was amplified using an electrical amplifier (ZHL-32A-S) and superimposed onto a dc current using a bias-T (Mini-circuits, ZFBT-4R2GW) to drive a LED (LUXEON Rebel ES LXML-PWC2). At the receiver, the intensity of the light signal was detected using a commercial photoreceiver (HCA-S200M-SI), and then captured by a sampling oscilloscope (Infinium, DSO8104A). Finally, the signal samples were downloaded and processed by MATLAB to recover the transmitted data.

Two types of DCO-OFDM signals were used: 4-QAM with a bias of 3dB and 16-QAM with a bias of 5dB. The received constellations are shown in Fig. 9 (a) and (e) and the constellations after channel equalization are shown in Fig. 9 (b) and (f). Using a ML detector, (which includes correction for shrinkage) give BERs of 1.57×10^{-4} for 4-QAM and 4.4×10^{-3} for 16-QAM. Applying our noise cancellation algorithm, reduces the noise significantly as shown in Fig. 9 (d) and (h), resulting in low BERs of 7.87×10^{-5} and 1.8×10^{-3} .

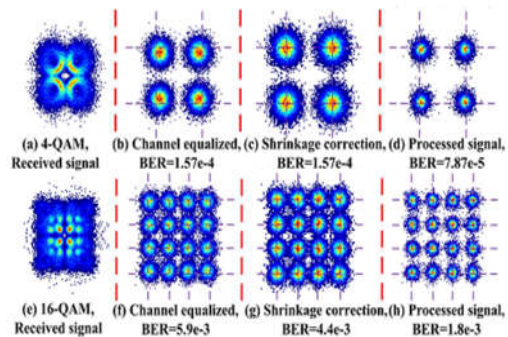


Fig. 9. Experimental results of the signal constellation.

RESULTS:

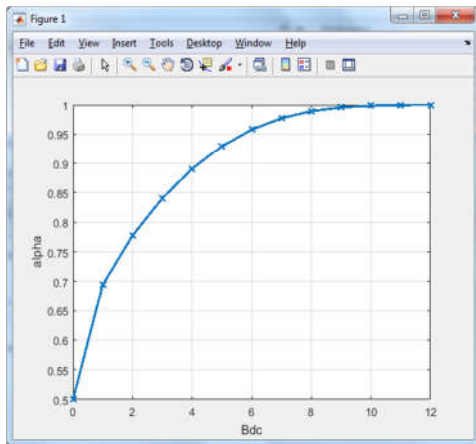


Fig.1. Attenuation versus bias level (dB).

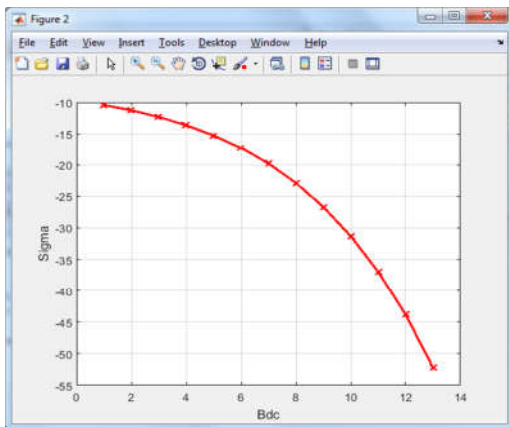


Fig.2. Clipping noise variance versus bias level (dB).

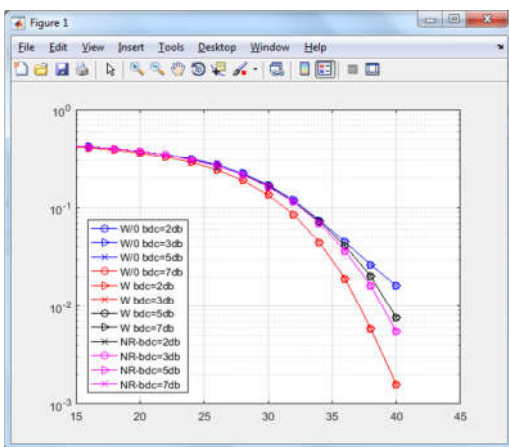


Fig. 3. Comparison between conventional receivers (with and without shrinkage correction) and clipping noise mitigation receiver using 4-QAM and 16-QAM.

V. CONCLUSION

In this paper, another collector based calculation is exhibited which applies a non-direct strategy to relieve the impact of section in optical OFDM frameworks. The calculation utilizes flag reproduction to gauge the flag at the transmitter before cut-out, and it can be executed for DCO-OFDM signals with both single-sided cutting and twofold side cut-out. Recreation and exploratory outcomes demonstrate that the new calculation can altogether diminish the BER.

REFERENCES

- [1] J. Armstrong, "OFDM for optical communications," *J. Lightw. Technol.*, vol. 27, no. 3, pp. 189–204, Feb. 1, 2009.
- [2] O. Gonzalez, R. Perez-Jimenez, S. Rodriguez, J. Rabadan, and A. Ayala, "OFDM over indoor wireless optical channel," *IEEE Proc.-Optoelectron.*, vol. 152, no. 4, pp. 199–204, Aug. 2005.
- [3] S. D. Dissanayake and J. Armstrong, "Comparison of ACO-OFDM, DCO-OFDM and ADO-OFDM in IM/DD systems," *J. Lightw. Technol.*, vol. 31, no. 7, pp. 1063–1072, Apr. 1, 2013.
- [4] D. Kim and G. L. Stübler, "Clipping noise mitigation for OFDM by decision-aided reconstruction," *IEEE Commun. Lett.*, vol. 3, no. 1, pp. 4–6, Jan. 1999.
- [5] J. J. Bussgang, "Crosscorrelation functions of amplitude-distorted Gaussian signals," *Res. Lab. Electron., Massachusetts Inst. Technol., Cambridge, MA, USA, Tech. Rep.*, Mar. 1952.
- [6] D. Dardari, V. Tralli, and A. Vaccari, "A theoretical characterization of nonlinear distortion effects in OFDM systems," *IEEE Trans. Commun.*, vol. 48, no. 10, pp. 1755–1764, Oct. 2000.
- [7] L. Chen, B. Krongold, and J. Evans, "Theoretical characterization of nonlinear clipping effects in IM/DD optical OFDM systems," *IEEE Trans. Commun.*, vol. 60, no. 8, pp. 2304–2312, Aug. 2012.
- [8] S. Dimitrov, S. Sinanovic, and H. Haas, "Clipping noise in OFDMbased optical wireless communication systems," *IEEE Trans. Commun.*, vol. 60, no. 4, pp. 1072–1081, Apr. 2012.